IOPscience iopscience.iop.org

Home Search Collections Journals About Contact us My IOPscience

GaInNAs-based vertical cavity semiconductor optical amplifiers

This article has been downloaded from IOPscience. Please scroll down to see the full text article.

2004 J. Phys.: Condens. Matter 16 S3345

(http://iopscience.iop.org/0953-8984/16/31/023)

View the table of contents for this issue, or go to the journal homepage for more

Download details:
IP Address: 129.252.86.83
The article was downloaded on 27/05/2010 at 16:23

Please note that terms and conditions apply.

INSTITUTE OF PHYSICS PUBLISHING JOURNAL OF PHYSICS: CONDENSED MATTER

J. Phys.: Condens. Matter **16** (2004) S3345–S3354 PII: S0953-8984(04)73711-X

GaInNAs-based vertical cavity semiconductor optical amplifiers

Dimitris Alexandropoulos and Mike J Adams

Electronics Systems Engineering Department, University of Essex, Wivenhoe Park, Colchester, Essex CO4 3SQ, UK

E-mail: dalexa@essex.ac.uk and adamm@essex.ac.uk

Received 12 December 2003
Published 23 July 2004
Online at stacks.iop.org/JPhysCM/16/S3345
doi:10.1088/0953-8984/16/31/023

Abstract

We explore the potential of GaInNAs-based vertical cavity semiconductor optical amplifiers (VCSOAs) operating at 1.3 μm. The obvious advantage of structural compatibility of GaInNAs active regions to GaAs/AlAs DBRs is accompanied by good predicted performance characteristics, comparable to published results on other material systems. We examine the potential of GaInNAs-VCSOAs to be operated as modulators both in transmission and reflection, and optimization schemes are discussed.

1. Introduction

The vertical cavity geometry of emitters has been the subject of extensive research in fabrication, characterization and modelling [1]. Recently, this has been extended to semiconductor amplifying structures [2]. The appealing characteristics of vertical cavity semiconductor optical amplifiers (VCSOAs) include [3] polarization insensitivity, superior fibre coupling efficiency and cost-effectiveness compared to edge emitting semiconductor optical amplifiers. Already the operation of InP-based VCSOAs at 1.3 μm [4] has been demonstrated using AlAs/GaAs distributed Bragg reflectors (DBRs). The drawback of this approach is that wafer fusion is needed, thus complicating the growth process.

A very promising alternative is the GaInNAs material system for active regions with AlAs/GaAs DBRs on GaAs substrates. This has motivated Calvez and co-workers [5], who have already demonstrated a GaInNAs-based VCSOA with a gain of 17.7 dB.

Our objective in this contribution is to study theoretically VCSOAs based on GaInNAs for operation at 1.3 μm. In doing so we will examine the performance of these on the basis of amplifier gain and we will extend our study to the prospects for the use of VCSOAs in schemes other than amplification, namely as modulators.

 © 2004 IOP Publishing Ltd Printed in the UK

2. VCSOA modelling

A comprehensive review of VCSOA modelling is presented in [6]. Here we summarize the basic mathematical framework for the sake of completeness. The modelling of VCSOAs has been based on two different approaches, namely the Fabry–Perot (FP) and the rate-equation (RE) methods. The two methods give the same unsaturated gain but fail to agree on the saturation properties of the amplifier. Royo and co-workers [7] have recently addressed this problem and proved that the two methods are equivalent provided that the definition of mirror losses is modified in the RE method. The important results of Royo and co-workers explain the discrepancies between the two methods for Fabry–Perot amplifiers presented in [8]. Here we follow the longitudinal averaged FP (LAFP) approach of Adams and co-workers [9] including the necessary changes to adapt to vertical geometry and the DBR structure.

After [9], the *average* signal photon density, $S_{\rm sig}$, and the average spontaneous photon density, $S_{\rm spon}$, are given respectively by

$$S_{\rm spon} = \left[\frac{(G_{\rm s}-1)[(1-R_{\rm b})(1+R_{\rm f}G_{\rm s})+(1-R_{\rm f})(1+R_{\rm b}G_{\rm s})]}{gL_{\rm c}(1-R_{\rm f}R_{\rm b}G_{\rm s}^2)} - 2\right]\frac{R_{\rm sp}N_{\rm g}}{gc} \tag{1}$$

$$S_{\rm sig} = \left[\frac{(G_{\rm s}-1)(1-R_{\rm f})(1+R_{\rm b}G_{\rm s})}{(1-\sqrt{R_{\rm f}R_{\rm b}}G_{\rm s})^2+4\sqrt{R_{\rm f}R_{\rm b}}G_{\rm s}\sin^2\Phi}\right]\frac{P_{\rm in}N_{\rm g}}{E\pi(W/2)^2L_{\rm c}gc} \tag{2}$$

where W is the aperture diameter, g is the modal gain, $G_{\rm s}$ is the single-pass gain, $N_{\rm g}$ the group refractive index, $P_{\rm in}$ the power of the input signal, E the energy of the signal, $R_{\rm sp}$ the total spontaneous emission rate, $R_{\rm f}$ the front mirror reflectivity and $R_{\rm b}$ the back mirror reflectivity. The phase Φ describes the detuning of the signal wavelength λ from the cavity resonance $\lambda_{\rm c}$ and is given by

$$\Phi = 2\pi n_{\rm c}L_{\rm c}\left(\frac{1}{\lambda}-\frac{1}{\lambda_{\rm c}}\right) \tag{3}$$

where $n_{\rm c}$ is the cavity refractive index and $L_{\rm c}$ the effective cavity length. The field penetrates significantly into the DBRs, altering the effective cavity length that the field propagates. The penetration depth is given by [10]

$$L_{\rm p} = \frac{\lambda_{\rm c}}{4n_{\rm c}}\frac{q}{1-p}\frac{(1-\alpha^2p^{2m-1})(1-p^{2m})}{1-q^2\alpha^2p^{4m-2}} \tag{4}$$

where p is the low-to-high refractive index ratio of the two layers of the DBR, q the low-to-high refractive index ratio of the first DBR interface and α that of the last DBR interface. Accounting for the penetration depth the effective cavity length is $L_{\rm c} = L_{\rm f}+L_m+L_{\rm b}$, with $L_{\rm f}$ and $L_{\rm b}$ the penetration depths of the front and back mirrors, respectively, and L_m the distance between the DBRs.

For the derivation of equations (1) and (2) it is assumed that the carrier density and hence the material gain is constant along the length of the active region of the amplifier. This approximation is poor for travelling-wave SOAs, but for VCSOAs, by virtue of the small length of the active region, it is sufficiently accurate.

Special care must be taken in positioning the quantum wells in the active region so that the gain regions have the maximum overlap with the standing wave pattern of the field. In this case the gain is enhanced by [11]

$$\xi = 1+\frac{\sin(2\pi n_{\rm c}L_{\rm stack}/\lambda_{\rm c})}{2\pi n_{\rm c}L_{\rm stack}/\lambda_{\rm c}}. \tag{5}$$

In the above expression $L_{\rm stack}$ is the thickness of each multi-quantum-well (MQW) stack.

The photon densities of 1 and 2 must satisfy the equation of charge conservation:

$$\frac{j}{eL_{\rm MQW}} = R_{\rm sp} + \frac{\xi T c}{N_{\rm g}}(g_{\rm m}(E_{\rm r})S_{\rm spon}(E_{\rm r})\beta(E_{\rm r}) + g_{\rm m}(E)S_{\rm sig}(E)) \quad (6)$$

where j is the current density, $E_{\rm r}$ the energy of the cavity resonance, $L_{\rm MQW}$ the total width of the quantum wells (QWs), e is the electron charge, β the spontaneous emission factor, Γ the longitudinal confinement factor defined by the ratio (active length)/(cavity length), and $g_{\rm m}$ the material gain.

The gains in transmission and reflection are given by [9]:

$$G_{\rm R} = \frac{(\sqrt{R_{\rm f}} - \sqrt{R_{\rm b}}G_{\rm s})^2 + 4\sqrt{R_{\rm b}R_{\rm f}}G_{\rm s}\sin^2\Phi}{(1-\sqrt{R_{\rm b}R_{\rm f}}G_{\rm s})^2 + 4\sqrt{R_{\rm b}R_{\rm f}}G_{\rm s}\sin^2\Phi} \quad (7)$$

$$G_{\rm T} = \frac{(1-R_{\rm f})(1-R_{\rm b})G_{\rm s}}{(1-\sqrt{R_{\rm b}R_{\rm f}}G_{\rm s})^2 + 4\sqrt{R_{\rm b}R_{\rm f}}G_{\rm s}\sin^2\Phi} \quad (8)$$

where $G_{\rm s}$ is the single-pass gain described by

$$G_{\rm s} = \exp[\xi g_{\rm m} L_{\rm MQW} - \alpha_{\rm cav} L_{\rm c}] \quad (9)$$

and $\alpha_{\rm cav}$ is the cavity loss. Examination of equations (7) and (8) provides some basic design rules [6]; in order to avoid lasing the relation $G_{\rm s}^2 R_{\rm f} R_{\rm b} < 1$ must be satisfied. This can be achieved either by tailoring the current and consequently altering $G_{\rm s}$, or by choosing appropriate values for $R_{\rm f}$ and $R_{\rm b}$. The amplifier gain drops below unity when $G_{\rm s}^2 < R_{\rm b}^{-1}$ since the emission through the back mirror exceeds the single-pass gain. We will use these conditions in section 3 when we calculate the minimum and maximum currents for a VCSOA. The maximum amplification gain is achieved when $\Phi = 0$ whereas the minimum occurs when $\sin\Phi = 1$.

3. 1.3 μm VCSOA characteristics

The theoretical description of the VCSOA structures is based on the self-consistent solution of equations (1)–(2) and (6)–(8). The material gain involved in the above equations is calculated based on free carrier theory, following the methodology presented in previous work [12], and involves the calculation of the bandstructure accounting for band mixing effects and the N-induced coupling of the bands. The β factor is calculated following the approach of Masum and co-workers [13]. A general description of the structure that we model is shown in figure 1 where the refractive index profile is shown. The figure serves the purpose of illustration and it is not to scale.

The active region is bounded by two dielectric mirrors of reflectivities $R_{\rm f}$ and $R_{\rm b}$. The length of the cavity is $3\lambda/2n_{\rm c}$ ($\lambda = 1.3\ \mu$m). Three stacks of $Ga_{0.65}In_{0.35}N_{0.025}As_{0.975}/GaAs$ QWs, each of 7 nm width, are positioned so that they have the maximum overlap with the standing-wave pattern of the field of the cavity. There are eight QWs in each MQW stack and the stacks are separated by $Al_{0.35}Ga_{0.65}As$ spacer material.

The DBR consists of pairs of AlAs/GaAs. In the present analysis we model the DBR stacks as hard mirrors [6], which enables the use of the FP equations presented above. The reflectivities are calculated numerically using a transfer matrix formulation [14]. Figure 2 shows the reflectivity of the DBR for various numbers of layers. Details for the calculations can be found in table 1. The usual trend of increasing peak reflectivity with number of layer pairs is exhibited.

Figure 3 shows the VCSOA gain in transmission and reflection for the structure of eight QWs per stack, outlined in table 1. The signal wavelength is $\lambda_{\rm s} = 1.3\ \mu$m and the structure is electrically pumped.

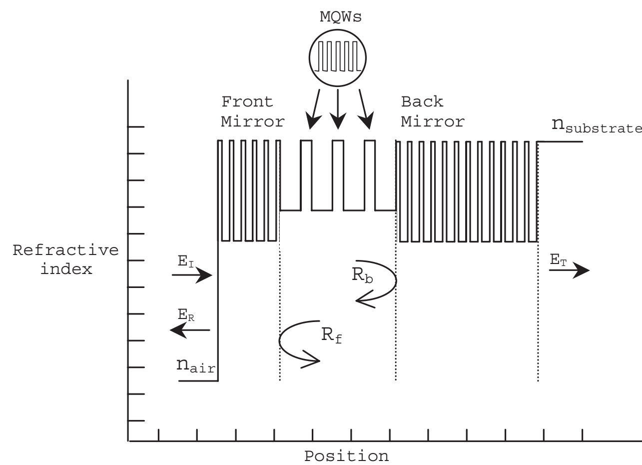

Figure 1. Description of a general VCSOA structure in terms of the real refractive index. E_I, E_R and E_T represent the incident, reflected and transmitted fields, respectively, and $n_{substrate}$ and n_{air} represent the refractive index of the substrate and air respectively.

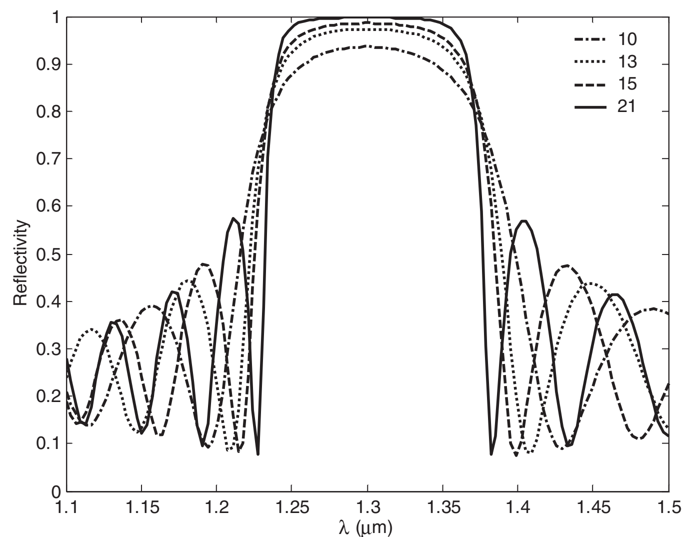

Figure 2. Reflectivity of AlAs/GaAs DBR for various numbers of pairs as indicated in the figure.

The minimum, I_{min}, and maximum current, I_{max}, are calculated numerically employing the conditions presented in section 2. For I_{max} we calculate the current for which the product $G_s^2 R_f R_b$ is *close* to unity for the sake of numerical convenience, hence I_{max} in the following must be interpreted as the current *just* below lasing condition. For the specific structure we calculate $I_{max} = 8.83$ mA and $I_{min} = 8.76$ mA which corresponds to approximately 99.2% of I_{max}. The very small range of currents is attributed to the high reflectivities of the VCSOA structure and to the fact that there are 24 QWs in the structure and therefore the differential gain is high.

The GaInNAs-VCSOA gain as predicted from our model has comparable values to the experimentally determined values for the GaInNAs-VCSOA (17.7 dB) [5] and InP-based

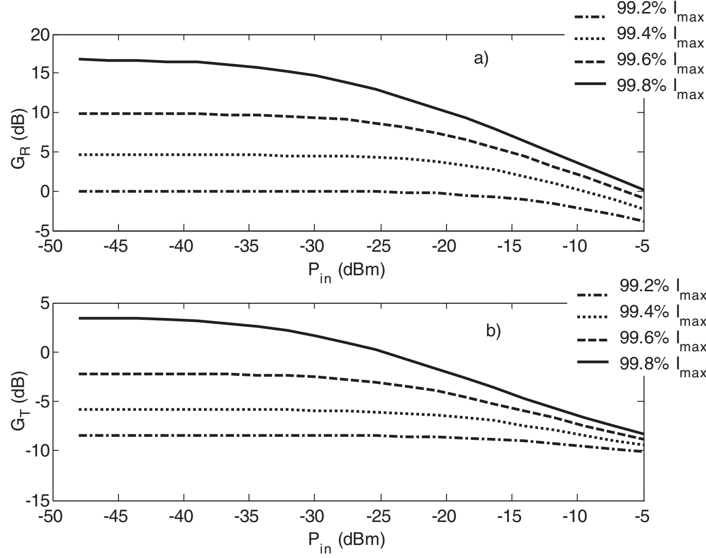

Figure 3. VCSOA gain in (a) reflection and (b) transmission of the structure of table 1 with eight QWs per stack, for various currents. The maximum current is calculated to be $I_{max} = 8.83$ mA.

Table 1. Details of the structures used in the computations.

Active material	$Ga_{0.65}In_{0.35}N_{0.025}As_{0.975}/GaAs$
α_{cav} (cavity loss)	15 cm^{-1}
N_g (effective refractive index)	4
A (monomolecular recombination coefficient)	2×10^8 s^{-1}
C (Auger recombination coefficient)	4×10^{-29} cm^6 s^{-1}
L_c (cavity length)	0.5821 μm
L_f (penetration depth of the front mirror)	0.5705 μm
L_b (penetration depth of the back mirror)	0.5674 μm
L_{spacer} (width of spacer material) for 4 QWs per MQW stack	0.053 μm
L_{spacer} (width of spacer material) for 8 QWs per MQW stack	0.015 μm
ξ (gain enhancement factor) for 4 QWs per MQW stack	1.688
ξ (gain enhancement factor) for 8 QWs per MQW stack	1.175
L_{MQW} (total width of the QWs) for 4 QWs per MQW stack	84 nm
L_{MQW} (total width of the QWs) for 8 QWs per MQW stack	168 nm
L_{stack} (thickness of each MQW stack) for 4 QWs	88 nm
L_{stack} (thickness of each MQW stack) for 8 QWs	164 nm
W (aperture diameter)	20 μm
α_{cav} (cavity losses)	15 cm^{-1}
n_c (cavity refractive index)	3.34
L_w (width of QW)	7 nm
R_b (back mirror reflectivity) for 26 pairs	0.999
R_f (front mirror reflectivity) for 15 pairs	0.985
n_{AlGaAs} ($Al_{0.35}Ga_{0.65}As$ refractive index)	3.285
n_{GaAs} (GaAs refractive index)	3.45
n_{AlAs} (AlAs refractive index)	2.89

VCSOA (14 dB) [4]. It is noted that in our results we have not accounted for fibre coupling losses. A more strict comparison is not possible as details of the structure in [5], such as compositions of the quantum wells, are not given.

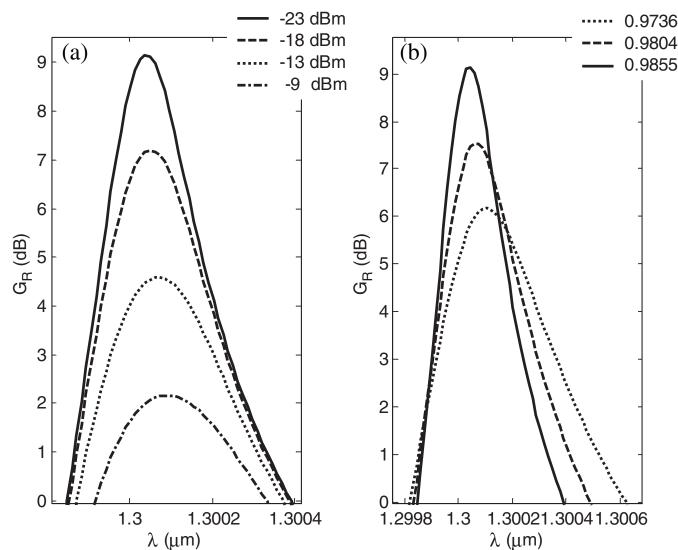

Figure 4. Amplifier gain for reflection against wavelength for (a) various P_{in} and $I = 8.80$ mA and (b) various R_f for $P_{in} = -23$ dB m and $I = 8.80$ mA.

The VCSOA reflected gain versus wavelength for different input powers and different reflectivities is shown in figures 4(a) and 4(b) respectively. The characteristics of the structure modelled here are summarized in table 1. The drive current for figure 4 is $I = 8.80$ mA. High input powers saturate the VCSOA leading to the suppressed gain values of figure 4(a). Lower reflectivities (figure 4(b)) favour high bandwidth at the expense of the peak gain value in agreement with [6].

The bandwidth for different input powers (figure 4(a)) ranges from 0.19 nm (−23 dB m) to 0.36 nm (−13 dB m) and for different reflectivities from 0.42 nm ($R_f = 0.9736$) to 0.19 nm ($R_f = 0.9855$). Although the trend agrees with [6] the magnitude lies between the values reported in the literature, namely 0.6 nm for InP-based VCSOAs [3] and 0.1 nm for GaInNAs-based VCSOAs [5].

4. Optimization issues

We have already referred briefly to how the reflectivities can be used to tune the amplifier bandwidth. An elaborate design and optimization study of VCSOAs has been performed by Piprek and co-workers [6]; hence we will avoid duplicating their results. However, their work focused on the cavity design rather than the active material itself and thus some comments regarding the active material are due. The design of the active material has been addressed in [15, 16] and the results outlined there can be extended to complete the design issue of VCSOAs. It was found that high In content and low N content (high compressive strain conditions) is the preferable growth-route for GaInNAs structures, as this enhances optical properties related to laser performance, such as gain, differential gain, transparency concentration etc. This design route is restrictive for edge emitting SOAs [17] because compressively strained QWs couple more efficiently to TE polarized radiation. On the other hand, because of the vertical geometry of VCSOAs, the inherent polarization insensitivity permits the use of highly strained GaInNAs/GaAs active regions which provide high gain and

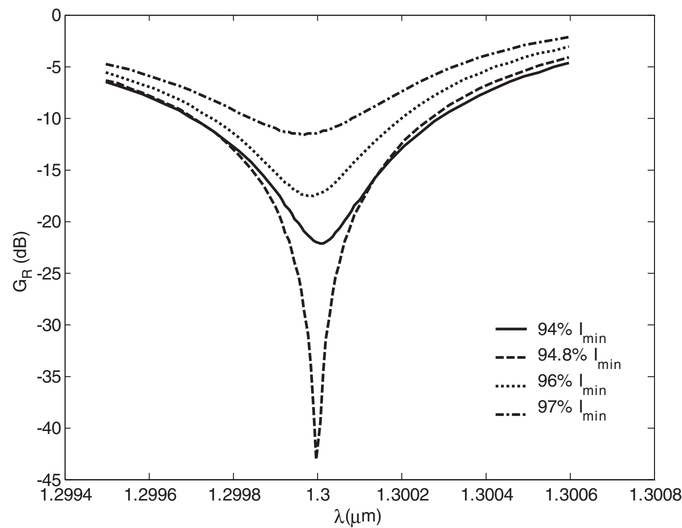

Figure 5. Gain in reflection for various currents for the structure described in the text. The calculated value of I_{min} is 1.10 mA.

have smaller requirements on drive currents. A more detailed optimization of the VCSOA design is beyond the scope of this paper.

5. VCSOAs as modulators

Apart from their apparent use for in-line amplification VCSOAs offer an interesting solution for modulation applications as, apart from the inherent gain dynamics, their geometry offers good coupling to optical fibre. Hence, it is not surprising that, despite the fact that the field of VCSOAs is relatively new, two groups have already demonstrated vertical cavity amplifying modulators (VCAMs) [18, 19]. In order to distinguish between the amplifying and modulating operation we will refer to these as VCAMs.

The VCAM can be realized either by operating the VCSOA in reflection or in transmission. The requirements in both cases are (a) that the amplifier in the ON state provides gain of approximately 5 dB and (b) the extinction ratio (ER), i.e. the ratio of the gain of the ON state to the gain of the OFF state, should be at least 25 dB.

First, we examine modulation in reflection. Figure 5 shows the gain in reflection versus wavelength for various currents. The structure contains four QWs per stack and the aperture diameter is 10 μm. The reflectivities are $R_{\mathrm{f}} = 0.964$ and $R_{\mathrm{b}} = 0.999$. For currents such that the VCSOA is in absorption a sharp negative resonance appears which is shifted to shorter wavelengths as the current is increased. For currents increasing further the resonance becomes positive. The negative resonance occurs only for operation in reflection and it can be understood with the help of equation (7); for sufficiently low currents G_{s} approaches the value of $(R_{\mathrm{f}}/R_{\mathrm{b}})^{1/2}$ and consequently the numerator of (4) tends to zero on resonance. It should be noted that this feature has been observed experimentally [19]. The condition $G_{\mathrm{s}} = (R_{\mathrm{f}}/R_{\mathrm{b}})^{1/2}$ along with single-pass gain for the wavelengths of figure 5 for the corresponding currents of that figure are plotted in figure 6. The reflectivities R_{f} and R_{b} are taken to be constant over the range of wavelengths of figure 6 which is justified by the plots of figure 2. At 94.8% of I_{min} the condition $G_{\mathrm{s}} = (R_{\mathrm{f}}/R_{\mathrm{b}})^{1/2}$ occurs close to the resonant wavelength. At the other currents this alignment does not occur hence the resonance is not so pronounced as shown in figure 5.

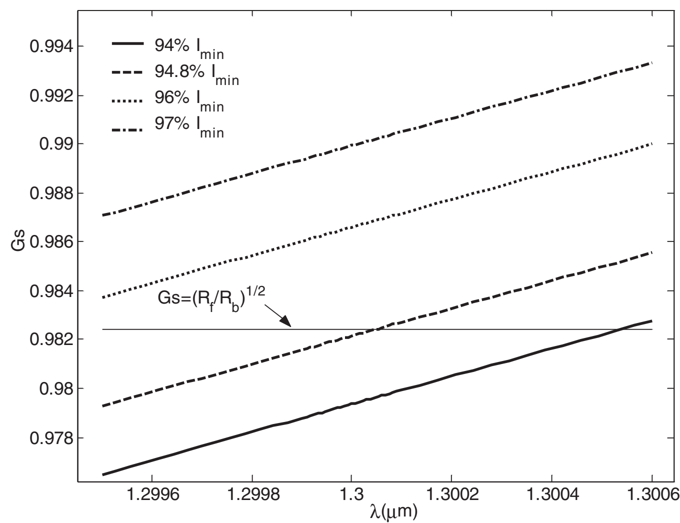

Figure 6. Single-pass gain against wavelength for various currents for the structure of figure 5. The condition $G_s = (R_f/R_b)^{1/2}$ is also plotted.

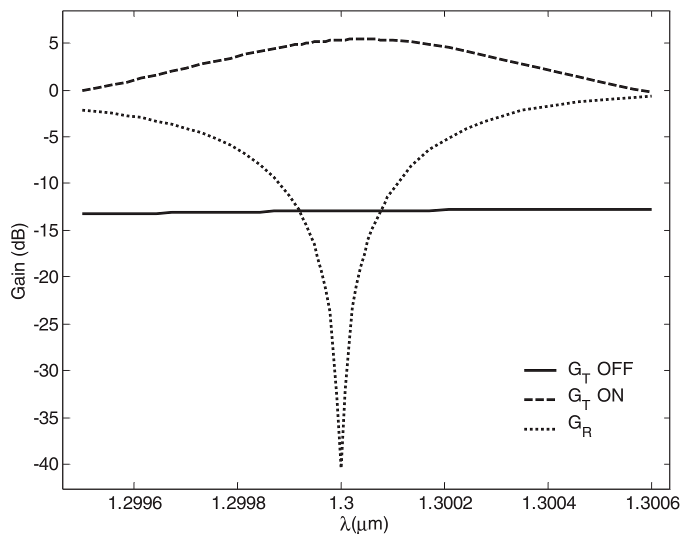

Figure 7. VCAM gain in transmission and reflection for the ON state and amplifier gain in transmission for the OFF state for the structure described in the text.

We note that the current can be used as a tuning parameter to enhance or suppress the resonance, for any given wavelength. Hence the negative feature can be tailored to improve the ER. By varying the current we can tune the single-pass gain to match the condition $(R_f/R_b)^{1/2}$ and thus achieve the suppression of the OFF state with a consequent improvement of the ER.

Application in reflection has the advantage that very high ER values can be obtained following the methodology outlined above. An alternative scheme to perform the modulating function is to operate the VCSOA in transmission. The characteristics of the VCAM in transmission are shown in figure 7. In the same figure we plot the amplifier gain in reflection.

It is desired that the amplifier gain in reflection be sufficiently suppressed so as to avoid the need for optical isolators, with consequent potential cost savings [20]. Tailoring the reflectivities of the structure we can ensure that the G_R is minimal. Here we have chosen $R_f = 0.985$ and $R_b = 0.952$; other than that the active region of the structure is the same as above. The drive current for the ON state is 1.16 mA whereas for the OFF state it is 0.827 mA.

The ER here is less than the corresponding value for VCAM operation in reflection. However, the advantage of this scheme is that the OFF state can be achieved with very low currents as opposed to the higher currents for VCAM in reflection. The disadvantages of VCAM operation in transmission are associated with practical device packaging aspects such as the difficulty of accurate alignment of the input and output fibres, and the problem of achieving good electrical contacts to a structure that must be transparent to the optical signal.

6. Conclusion

The potential of GaInNAs-VCSOAs has been highlighted by means of the comparable performance characteristics with published results on other material systems. We examined in detail the suggested operation of GaInNAs-VCSOAs in modulators. The drive current for the OFF state can be used to greatly improve the ER when the VCAM is operated in reflection. For operation in transmission the ER is expected to have lower values than when the VCAM is operated in reflection, but the current for the OFF state does not need to be accurately specified. The reflected gain of the ON state can be effectively suppressed by choosing carefully the reflectivities and current of operation. In this way the VCAM structure is greatly simplified with subsequent cost reduction. It should be noted that the methods presented here regarding the manipulation of the VCAM are not restricted to GaInNAs-based VCAMs and are directly applicable to VCAMs that utilize other gain materials. In conclusion, this work, combined with our earlier work on the tailoring of the material properties of GaInNAs-based optoelectronic devices [15, 17], provides the framework for the design of GaInNAs-based VCSOAs.

References

[1] Wilmsen C, Temkin H and Coldren L A (ed) 1999 *Vertical-Cavity Surface-Emitting Lasers* (Cambridge: Cambridge University Press)

[2] Tombling C, Saitoh T and Mukai T 1994 Performance predictions for vertical cavity semiconductor laser amplifiers *IEEE J. Quantum Electron.* **30** 2491–9

[3] Karim A, Steffan Bjorlin E, Piprek J and Bowers J E 2000 Long wavelength vertical-cavity lasers and amplifiers *IEEE J. Sel. Top. Quantum Electron.* **6** 1244–53

[4] Steffan Bjorlin E, Riou B, Abraham P, Piprek J, Chiu Y-J, Alexis Black K, Keating A and Bowers J E 2001 Long wavelength vertical-cavity semiconductor optical amplifiers *IEEE J. Quantum Electron.* **37** 274–81

[5] Calvez S, Clark A H, Hopkins J M, Macaluso R, Merlin P, Sun H D, Dawson M D, Jouhti T and Pessa M 2003 1.3 μm GaInNAs optically-pumped vertical cavity semiconductor optical amplifier *Electron. Lett.* **39** 100–1

[6] Piprek J, Bjorlin S and Bowers J E 2001 Design and analysis of vertical-cavity semiconductor optical amplifiers *IEEE J. Quantum Electron.* **37** 127–34

[7] Royo P, Koda R and Coldren L A 2002 Vertical cavity semiconductor optical amplifiers: comparison of Fabry–Perot and rate equation approaches *IEEE J. Quantum Electron.* **38** 279–84

[8] Ghafouri-Shiraz H 1996 *Fundamentals of Laser Diode Amplifiers* (Chichester: Wiley)

[9] Adams M J, Collins J V and Henning I D 1985 Analysis of semiconductor laser optical amplifiers *IEE Proc.* J **132** 58–63

[10] Babic D I and Corzine S W 1992 Analytic expressions for the reflection delay, penetration depth, and absorptance of quarter-wave dielectric mirrors *IEEE J. Quantum Electron.* **28** 514–24

[11] Corzine S W, Geels R S, Scott J W, Yan R H and Coldren L A 1989 Design of Fabry–Perot surface-emitting lasers with a periodic gain structure *IEEE J. Quantum Electron.* **25** 1513–24

[12] Alexandropoulos D and Adams M J 2002 Gain, differential gain and linewidth enhancement factor of GaInNAs/GaAs strained quantum wells *J. Phys.: Condens. Matter* **14** 3523–36
[13] Masum J, Ramoo D, Balkan N and Adams M J 1999 Temperature dependence of the spontaneous emission factor in VCSELs *IEE Proc. Optoelectron.* **146** 245–51
[14] Yeh P and Yariv A 1984 *Optical Waves in Crystals: Propagation and Control of Laser Radiation* (New York: Wiley)
[15] Alexandropoulos D and Adams M J 2003 Design considerations for 1.3 μm emission of GaInNAs/GaAs strained quantum well lasers *IEE Proc. Optoelectron.* **150** 105–9
[16] Alexandropoulos D and Adams M J 2003 Assessment of GaInNAs as a potential laser material *IEE Proc. Optoelectron.* **150** 40–44
[17] Alexandropoulos D and Adams M J 2003 Theoretical study of GaInNAs based semiconductor optical amplifiers *IEEE J. Quantum Electron.* **39** 647–55
[18] Bouche N, Corbett B and Kuszelewicz R 1996 Vertical-cavity amplifying photonic switch at 1.5 μm *IEEE Photon. Technol. Lett.* **8** 1035–7
[19] Bjorlin E S, Dahl A, Piprek J, Abraham P, Chiu Y J and Bowers J E 2001 Vertical-cavity amplifying modulator at 1.3 μm *IEEE Photon. Technol. Lett.* **13** 1271–3
[20] Suzuki N, Ohashi M and Nakamura M 1997 A proposed vertical-cavity optical repeater for optical inter-board connections *IEEE Photon. Technol. Lett.* **9** 1149–51